Team One Report

Rachel Marbaker

Video created with Tandralee Chetia and Riley Mente

MCEN 5151-002 Flow Visualization
6 October 2023

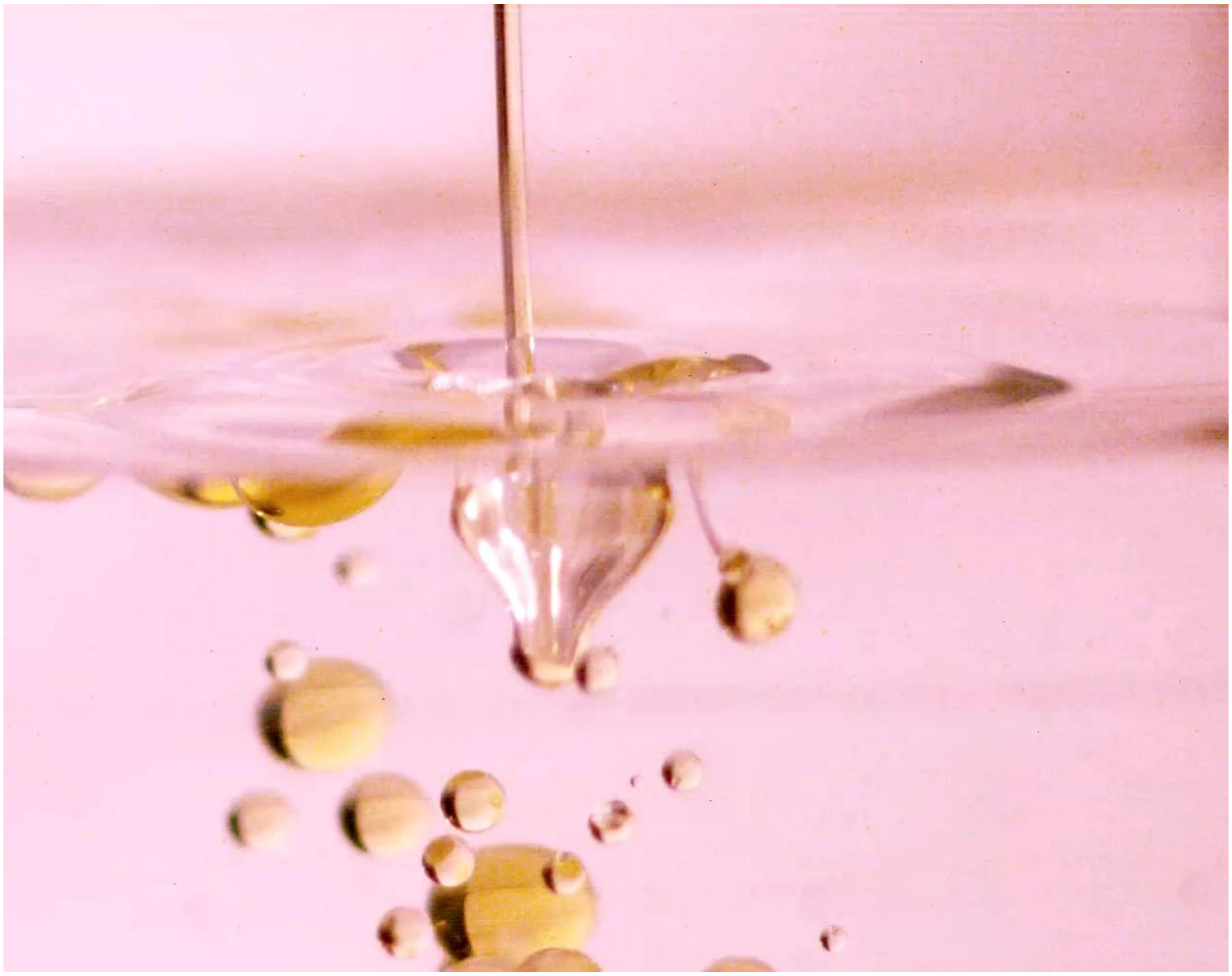

Thumbnail for video, entitled Hydrophobia

Purpose and context

This image was taken for the Team 1 assignment in Flow Visualization (Fall 2023, MCEN 5151) with Professor Hertzberg. The end goal for the assignment was an image that artistically demonstrated a fluid phenomenon. My team initially intended to use the high-speed camera to film the formation of alginate beads in calcium chloride solution. As part of setting up for that process, we practiced focusing the image on the surface of water and tested the high-speed camera for both water and oil pours. All of us ultimately selected images from these two “practice” set ups because it was challenging to get clearly defined boundaries in the alginate images. Unfortunately, the final product has some limitations associated with its informal data imaging. The video submitted for this assignment, titled Hydrophobia, shows the surface interactions as oil is poured into water.

Materials and methods (flow apparatus)

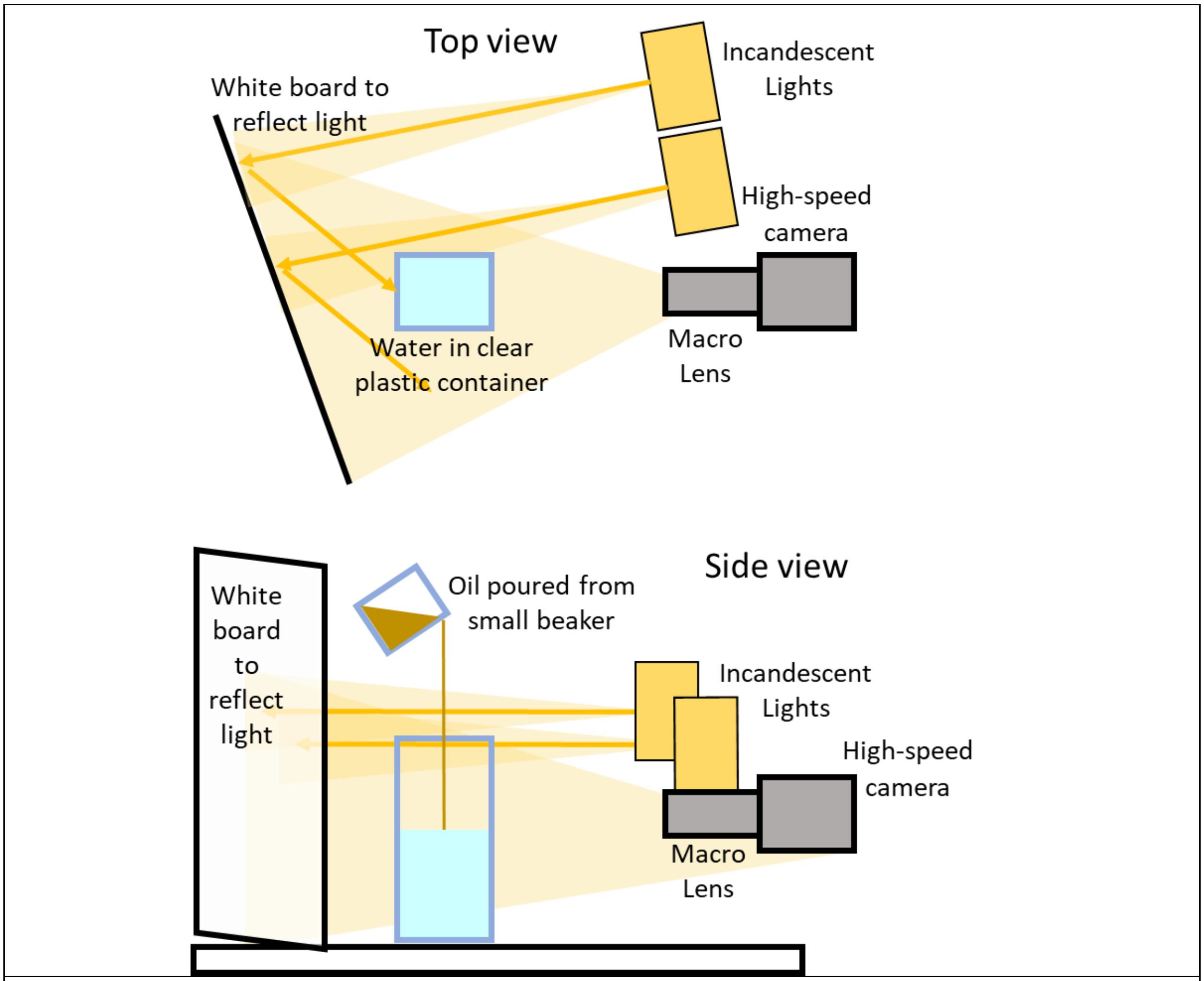

Figure 1: Flow visualization set up from above (top) and from the side (bottom). The high speed camera with attached macro lens was set up directly facing and level with the surface of the water in the plastic container. Incandescent lights were offset vertically and horizontally to reduced glare. A white board was positioned behind the container and at an offset to reflect light. The clear plastic container was partially filled with water and the camera was adjusted to focus on the water surface. Oil was poured into the center of the water container from a small beaker.

The flow apparatus is illustrated in Figure 1. The set up is arranged around a plastic container (10 cm x 10 cm x 25 cm) half filled with water. The high-speed camera (Phantom C110) fitted with a macro lens (Micor-NIKON 105 mm) on a macro extension tube (N-AF Zeikos Digital AF) was positioned approximately level with the surface of the water about 0.6 m from the center of the water container. The camera was focused manually using a bottle partially submerged in the water, so that text from the label appeared sharp both above and below the water surface. Two incandescent work lights (500 watts; 7500 lumens [1]) were positioned adjacent to the camera and angled slightly above and to the side of the water container. A white board was positioned at a slight angle behind the water container to reflect the light.

The Phantom C110 high-speed camera was controlled using proprietary software called Phantom Camera Control (PCC) 2.8. which was connected to the camera using an ethernet cable. The software was used to trigger and stop the imaging. The camera frame rate was 1215 frames per second and resulted in images 768 x 768 pixels [2]. The camera was triggered before the pour began. The oil (Pompeian Smooth Extra Virgin Olive Oil) was poured by hand from a small beaker positioned just above and centered on the plastic container. The oil traveled approximately 15 cm before hitting the surface of the water. Approximately 30 ml of oil was poured over about 10 seconds for a flow rate of about 3 ml/s. Approximating an oil stream diameter of 2mm, we calculate the flow velocity as 0.955 m/s.

Fluid Dynamics

The poured oil remains in an even narrow stream until it hits the surface of the water. At contact, the inertia of the oil stream pressed the surface of the water downward. In the initial impact, as the surface of the water gives but the surface tension remains unbroken, the oil creates an air pocket (Figure 2a). At the base of the air pocket, where the potential energy generated in the pour is counteracted and then overwhelmed by the buoyancy force, the oil begins to curl upward in small vortices. Droplets of oil spiral out of those vortices and form neat spheres that interact with the stream as they rise to the surface (figure 2b). These interactions create shape changes, breaks in the stream, and lensing. Larger spheres of oil rise faster and the droplets collect on the surface, eventually bursting so that a layer of oil globes becomes a smooth film (figure 2c).

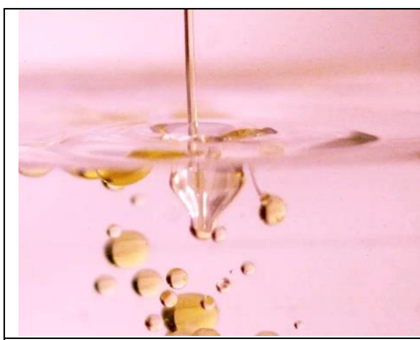	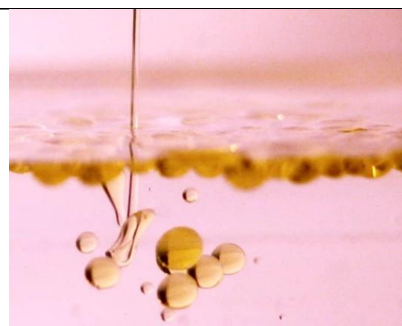	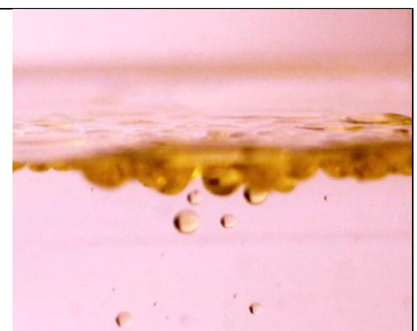
Figure 2 a Air pocket forming at the impact of the oil stream.	B Small vorticities spiraling off the base of the oil stream.	C Oil droplets coalescing on the water surface and eventually bursting to form a thin film of oil.

For the oil-water interaction in the video, the phenomena at play are surface tension, immiscibility, and buoyancy.

Impact, surface tension, and vortices: Poured from above, the oil stream impacts the surface of the water with the inertia of the stream concentrated on a small impact area. This initial impact pushes the water down, but there was a delay as pressure built before the water's surface tension was broken. During the pour, the oil traps some air below the stream, creating a thin film of air between the oil and water at impact [3]. Since the oil drop is then exerting pressure on the air which is exerting pressure on the water, the low density air is accelerating both oil (slowing down) and water (speeding up), both fluids of higher density [3]. Thus, the Rayleigh-Taylor instability as well as a kind of air-film rupture reminiscent of a popping bubble contribute to the formation of the air pocket and influence the eventual surface tension rupture [3]. The stream of oil did not create a rebounding jet, but formed an impact crater and broke the surface without splash. This behavior is consistent with a low Weber number, which indicates that drag and cohesion forces have similar magnitudes[4]–[6]. The Weber number represents the ration of drag forces over cohesive forces as

$$We = \frac{drag}{cohesion} = \frac{\rho v^2 l}{\sigma}$$

where ρ is the density of fluid (water[7]), v is the velocity (of the falling oil), l is the characteristic length, taken here to be the diameter of the stream (approximately 2 mm), and σ, the surface tension[5]. Accordingly, we get

$$We = \frac{(998kg/m^3)(0.955m/s)^2(0.002m)}{72.8e - 3\ N/m} = 26.18.$$

This Weber number is near where we anticipate coalescence of the oil in water which would prevent the jet [4], but the jet is also prevented by the continuous stream. When the stream breaks into droplets near the end of the pour, we observe the formation of small jets.

In miscible fluids, coalescence generates small vortex rings, but in immiscible fluids these may not appear [4], [8]. However, the nature of the oil accelerating water is, similar to the formation of the air pocket, characteristic of the Raleigh-Taylor instability which produces vortices and may also instigate a Kelvin-Helmholtz instability with further vortices [9]. This, in addition to the visible formation of small mushroom shapes as the oil decelerated against the water, suggest the formation of vortices spinning off the stream and initiating the formation of small globules of oil.

Immiscibility: Olive oils is made up of three fatty acids, each headed by a carboxyl group [10]. While olive oils may contain many different combinations of fatty acids, the International Council of Olive Oil “encourages growers to select cultivars…that have the highest levels of monosaturated oleic acid” [10]. An analysis of fatty acids generated by *Fusarium*, a fat-producing fungi, unsaturated fats such as oleic acid are more polar[11]. This fits nicely with most familiar explanation of oil’s immiscibility in water, which relies on the concept of polar and nonpolar bonds. In this explanation, the nonpolar bonds of the fatty acid chains in the oil cluster together with the slightly more polar carboxyl heads interfacing with the polar water molecules. However, analysis of this explanation in terms of enthalpy (ΔH, referring to the change of heat energy in a system [12]), shows that the change in enthalpy for mixing an oil and water solution is near 0 [13]. Instead the immiscibility is driven by entropy [13], [14]. Since there are many similar arrangements of bulk water molecules with short lived polar bonds and continuous molecular movment, water has high entropy [14]. Furthermore, these water molecules are dwarfed by the triglyceride oil molecules [10], [13]. Incorporating large lipid molecules into the water results in entropy loss by reducing the free movement of the water molecules [13], [14]; thus, water and oil don’t mix because of the infinitesimally low probability of entropy reduction and we observe the formation of oil globules as vortices spin off the oil stream.

Buoyancy: Because oil is less dense than water (895 kg/m^3 compared to water's 998 kg/m^3 [7], [15]), the force of displaced water pushes the oil globules up toward the surface. Larger globules displace more water, resulting in greater buoyancy and less susceptibility to molecular interactions and rise to the surface more rapidly. During the rising process, we observe some lensing effects from the oil sphere magnifying the stream behind it. Upon reaching the surface, the oil globules sit partially submerged. Larger globules burst after a moment, forming a thin film on top of the water rather than partially submerged[16], [17]. After a longer delay, smaller globules also burst. The globules are initially held together by cohesion but the buoyancy force from the water on the submerged part of the bubble is soon acting against the surface tension of the oil in the air (Figure 3).

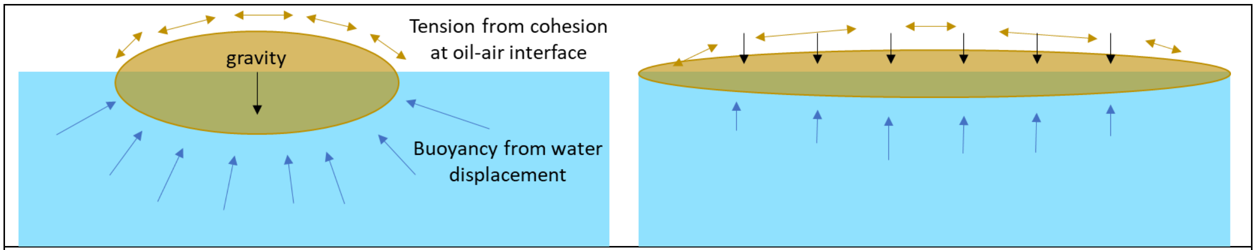

Figure 3: Forces on an oil globule and the changed forces in an oil film.

Imaging technique

The .mp4 video file was generated from still photos taken at 1215 frames per second using a Phantom C110 high-speed camera fitted with a Micro-NIKON 105 mm macro lens on a N-AF Zeikos Digital AF 36 mm extension tube. The camera lens was positioned level with the surface of the water manually focused. Light from two incandescent work lights was reflected against a whiteboard to illuminate the fluid with minimal glare.

The camera was triggered before the pour using Phantom Camera Control (PCC) 2.8 and took images at 1215 fps until the pour was finished and the camera stopped using the PCC software. This frame rate resulted in images 768 x 768 pixels [2]. Aperture was not recorded. ISO was not available.

Table 1. Camera settings

Camera settings	**Sony α6000** (ILCE-6000)
Focal length	141 mm
Exposure time	1/1215 second
Pixels	756x756
Lens	**SEL50F18**
Micro-NIKON	105mm
N-AF Zeikos Digital AF Extension tube	36 mm

Post-processing was completed in MiniTool Movie Maker. Using this tool, the video was cropped slightly to move the surface of the water slightly upwards in the frame. In this crop, the aspect ratio was changed from 1:1 to 4:3, theoretically taking the pixels of the image from 768 x 768 to 768 x 576. The exported .mp4 is resampled and has an frame width of 1440 x 1080 pixels. The video was also cropped temporally to remove time before the pour began and after the pour concluded and is played back at

0.5x speed of the .mp4 exported from PCC (I was unable to find the playback rate of the export). Music was added: the track is titled Island Beats by Arulo and was downloaded royalty free from Mixkit.com.

Colors were changed slightly by increasing the contrast (100) and brightness (7.3) and a comparison is included in figure 4.

	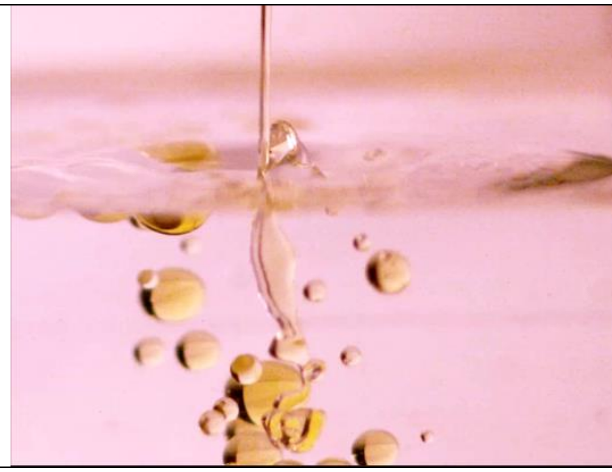
Figure 4: Before post processing	After post processing, including a slight change in aspect ratio, increased contrast and brightness.

Image reflection

Because of the huge size of the high-speed camera data files, the data was drastically compressed in the PCC software to export an .mp4, a known lossy format. For this reason, the video I am working with is far lower quality than the one I was viewing on the PCC software. I further compounded this quality loss by cropping the video which resampled the pixels further and I will update the format of my FlowVis.org submission to remove this secondary loss. I also wish we had been able to rearrange the lens and extension tube configuration (we were not due to linkage compatibility) because the narrow depth of field limits the observable phenomena. I also wish we had adjusted the framing to consistently capture the full depth of the stream.

Even so, I like the motion of the flow and the way I was able to match the bounce of the music with the oil bubble formation. The pale pink light artifact contrasts nicely with the golden color of the oil and gives the visual a consistent warmth. Both the visual and the fluid phenomenon in the video seem simple because they are familiar. When slowed down, when examined more deliberately, the complexity becomes apparent. There are patterns, repetitions, but they are imperfect copies. Interactive scenarios of the oil spheres with the oil stream and the swirling water play out repeatedly, but never the same choreography twice.

Sources

[1] “Watts to lumens (lm) conversion calculator.” Accessed: Oct. 05, 2023. [Online]. Available: https://www.rapidtables.com/calc/light/watt-to-lumen-calculator.html

[2] "PHANTOM Miro C110 High-Speed Camera," Darwin Microfluidics. Accessed: Oct. 05, 2023. [Online]. Available: https://darwin-microfluidics.com/products/phantom-miro-c110-high-speed-camera

[3] J. Sigler and R. Mesler, "The behavior of the gas film formed upon drop impact with a liquid surface," *J. Colloid Interface Sci.*, vol. 134, no. 2, pp. 459–474, Feb. 1990, doi: 10.1016/0021-9797(90)90156-I.

[4] M. Rein, "Phenomena of liquid drop impact on solid and liquid surfaces," *Fluid Dyn. Res.*, vol. 12, no. 2, pp. 61–93, Aug. 1993, doi: 10.1016/0169-5983(93)90106-K.

[5] "Surface and Interfacial Tension - Nanoscience Instruments." Accessed: Oct. 06, 2023. [Online]. Available: https://www.nanoscience.com/techniques/tensiometry/surface-interfacial-tension/

[6] "Weber number," *Wikipedia*. May 30, 2022. Accessed: Oct. 06, 2023. [Online]. Available: https://en.wikipedia.org/w/index.php?title=Weber_number&oldid=1090654680

[7] "Water Density | U.S. Geological Survey." Accessed: Oct. 06, 2023. [Online]. Available: https://www.usgs.gov/special-topics/water-science-school/science/water-density

[8] "V. On the formation of vortex rings by drops falling into liquids, and some allied phenomena." Accessed: Oct. 06, 2023. [Online]. Available: https://royalsocietypublishing.org/doi/epdf/10.1098/rspl.1885.0034

[9] A. Sedaghat and S. Mokhtarian, "Numerical Simulation of Rayleigh-Taylor Instability," vol. 6, no. 1, 2013.

[10] R. Mailer, "Chemistry and quality of olive oil".

[11] H. S. Murali, M. S. Mohan, K. S. Manja, and R. Sankaran, "Polar and nonpolar lipids and their fatty acid composition of a fewFusarium species," *J. Am. Oil Chem. Soc.*, vol. 70, no. 10, pp. 1039–1041, Oct. 1993, doi: 10.1007/BF02543034.

[12] *Enthalpy: Crash Course Chemistry #18*, (Jun. 17, 2013). Accessed: Oct. 06, 2023. [Online Video]. Available: https://www.youtube.com/watch?v=SV7U4yAXL5I

[13] T. P. Silverstein, "The Real Reason Why Oil and Water Don't Mix," *J. Chem. Educ.*, vol. 75, no. 1, p. 116, Jan. 1998, doi: 10.1021/ed075p116.

[14] *Why don't oil and water mix? - John Pollard*, (Oct. 10, 2013). Accessed: Oct. 06, 2023. [Online Video]. Available: https://www.youtube.com/watch?v=h5yIJXdItgo

[15] M. S. Sarjadi, T. C. Ling, and M. S. Khan, "Analysis and comparison of olive cooking oil and palm cooking oil properties as biodiesel feedstock," *J. Phys. Conf. Ser.*, vol. 1358, no. 1, p. 012007, Nov. 2019, doi: 10.1088/1742-6596/1358/1/012007.

[16] Corcorran, Pinksy, Wilson, Parker, "Thin Film Interference." Accessed: Oct. 06, 2023. [Online]. Available: http://outreach.phys.uh.edu/chemexperiments.htm

[17] J. A. Fay, "PHYSICAL PROCESSES IN THE SPREAD OF OIL ON A WATER SURFACE".